

# Effects of substrate nonlinear deformation on the wrinkling pattern transition in hyperelastic bilayer systems†

Yan Zhao<sup>1</sup>, Yanping Cao<sup>1\*</sup>, Wei Hong<sup>2</sup>, M. K. Wadde<sup>3</sup>, Xi-Qiao Feng<sup>1</sup>

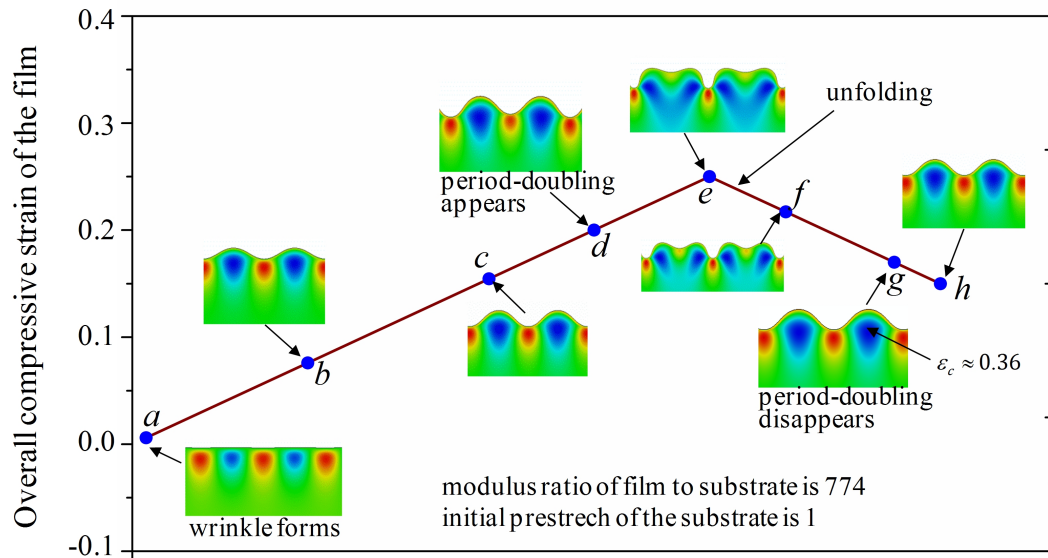
<sup>1</sup>AML & CNMM, Institute of Biomechanics and Medical Engineering, Department of Engineering Mechanics, Tsinghua University, Beijing 100084, China

<sup>2</sup>Department of Aerospace Engineering, Iowa State University, Ames, IA 50011, USA

<sup>3</sup>College of Engineering, Mathematics and Physical Sciences, University of Exeter, North Park Road, Devon EX4 4QF.

† Electronic supplementary information (ESI) available. See DOI:

## Table of contents entry



Wrinkling pattern evolution in a hyperelastic bilayer system engendered by compression. When period-doubling mode occurs, the maximum nominal **compressive** strain along the loading direction is about 0.36 (point g), which is defined as the characteristic strain and adopted to develop explicit solutions for the critical condition of period-doubling wrinkling.

\*Corresponding author: Tel.: +86 10 62772520; fax: +86 10 62781824.

Email address: [caoyanping@tsinghua.edu.cn](mailto:caoyanping@tsinghua.edu.cn) (Y. P. Cao)

**Abstract:** Compression of a stiff film on a soft substrate will first lead to surface wrinkling when the compressive strain reaches a critical value. Further compression may cause a wrinkling-folding transition, and the sinusoidal wrinkling mode gives way to a period-doubling bifurcation. The onset of the primary bifurcation has been well understood, but a quantitative understanding of the secondary bifurcation remains elusive. Our theoretical analysis of the branching of surface patterns reveals that the wrinkling-folding transition depends on the wrinkling strain and the prestrain in the substrate. A characteristic strain in the substrate is uncovered to determine the correlation among the critical strain of period-doubling mode, the wrinkling strain and the prestrain in an explicit form. This characteristic strain is close to the critical strain for the onset of sulcus at the surface of a compressed hyperelastic solid, indicating that the nonlinear instability of the substrate plays a key role. The results reported here on the one hand provide a quantitative understanding of the wrinkling-folding transition observed in natural and synthetic material systems and on the other hand pave the way to control the wrinkling mode transition by regulating the strain state in the substrate.

## 1. Introduction

Surface instability is frequently observed in squeezed soft materials.<sup>1-6</sup> The physics of this nonlinear phenomenon could be harnessed to create tunable patterns, to fabricate functional surfaces, and to understand the correlation between growth and morphogenesis in some natural systems. Therefore, it has received considerable attention of many scientists and engineers.<sup>7-13</sup> Biot<sup>14</sup> made a pioneering effort to understand surface instability of a neo-Hookean solid subject to plane-strain compression. His linear perturbation analysis leads to a critical compressive (nominal) strain of 45.6% for the onset of surface instability. Recent analysis<sup>12</sup> based on Koiter's elastic stability theory reveals that surface wrinkling of a neo-Hookean solid is highly unstable **due** to the nonlinear interaction among the multiple modes associated with the critical compressive state. Concomitantly, wrinkling is sensitive to exceedingly small initial imperfections and spontaneously collapses into a local crease. The nonlinear analysis of Hong et al.<sup>7</sup> and Hohlfeld and Mahadevan<sup>9</sup> indicated that crease/sulcus represents a subcritical instability mode, which is energetically favorable when the nominal compressive strain is beyond 35.4%. Surface instability of a stiff film resting on a soft substrate (bilayer system) is usually believed to be fundamentally different from that of a hyperelastic solid. In the former, surface wrinkles are rather stable, especially when the modulus ratio of the film to substrate is large, and could be reliably observed over a wide loading range.<sup>13</sup> This paper is concerned with an interesting experimental phenomenon observed by Brau et al.<sup>5</sup> in PDMS film/substrate systems, as shown in Fig. 1. They reported that the sinusoidal

wrinkling mode will transform to the period-doubling mode when the overall compressive strain reaches around 19%. This phenomenon was recently confirmed by nonlinear finite element simulations.<sup>10</sup> Moreover, the nonlinear analysis reveals that the critical condition for the onset of the wrinkling pattern transition largely depends on the nonlinear deformation behavior of the substrate. Precompression favors the occurrence of the folding and prestretch will retard the wrinkling mode transition; over prestretch may lead to the mountain ridge mode.<sup>11</sup> Hutchinson<sup>13</sup> investigated the role of substrate nonlinearity on the wrinkling of thin films bonded to a compliant substrate within the initial post-bifurcation range when wrinkling first emerges. His insightful analysis revealed that when the elastic modulus of the film is about five times greater than that of the substrate, the wrinkling bifurcation will be stable, while for a relatively soft film, the wrinkles can be unstable. However, the initial post-bifurcation expansion does not capture the unusual wrinkling modes observed at compressive strains well above the bifurcation strain such as period doubling, folding<sup>5,12,15</sup> and ridging<sup>11,16</sup>. These previous studies<sup>5-16</sup> help us to understand the physics behind the wrinkling pattern evolution in hyperelastic bilayer systems. However, a quantitative understanding of the wrinkling mode transition from sinusoidal to period-doubling in bilayer systems with the presence of substrate pre-deformation remains elusive.

This paper is organized as follows. Theoretical analysis is first performed in Section 2 on the branching of the wrinkling mode to characterize the correlation between the wrinkling transition strain and the parameters in the system.

Computational studies are carried out in Section 3 to explore the deformation behavior of the substrate in the vicinity of the second bifurcation point. A characteristic (nominal) strain in the substrate is uncovered at the occurrence of the period-doubling mode. In Section 4, explicit solutions are given to predict the critical overall strain for the onset of the period-doubling mode in the cases with and without substrate pre-deformation. Section 5 gives some concluding remarks.

## 2. Theoretical analysis of wrinkling pattern transition

### 2.1 Model

To determine the critical compressive strain for the onset of a period-doubling mode, we first perform a theoretical analysis on the wrinkling mode branching. For the system illustrated in Fig. 2, we explore displacement controlled loading procedure. The upper surface of the thin film is traction-free. Here  $x$  is coordinate of the initial configuration.  $l$  and  $h$  are the length and thickness of the film, respectively, and  $l$  is assumed to be much larger than the wrinkling wavelength of the system. **We assume that the film follows the generalized Hooke's law and the substrate is an incompressible neo-Hookean material.** The overall compressive strain in the film in the fundamental state is  $\delta$ . In the case of plane strain, the resultant membrane stresses in the film in the fundamental state can be obtained by

$$N_{xx} = -\sigma h, \quad N_{yy} = -\nu\sigma h, \quad N_{xy} = 0, \quad (1)$$

**where  $\sigma = \bar{E}\delta$  and  $\bar{E} = E/(1-\nu^2)$ , with  $E$  and  $\nu$  being the Young modulus and Poisson's ratio, respectively.**

The nonlinear von Karman plate equations<sup>17-19</sup> are used to model the film in the wrinkling state (Fig. 2):

$$\frac{1}{12} \bar{E} h^3 w_{,xxxx} = F_{,yy} w_{,xx} - R - h \sigma w_{,xx} , \quad (2a)$$

$$\frac{1}{Eh} \nabla^4 F = 0 \quad (2b)$$

where  $w(x)$  is the additional deflection of the film from the fundamental state.  $F$  is the stress function and

$$R = R_0 + Kpw + K_2 (pw)^2 + \dots \quad (3)$$

refers to a Taylor expansion of the resistant force of the foundation to the film.  $R_0$  is

the constant term of  $R$ . If the expansion is up to the linear term,  $R_0$  is zero, ensuring

that the total vertical resistant force is zero.  $R_0$  may be nonzero for a nonlinear

foundation, but it can be seen from subsequent analysis that  $R_0$  has no contribution to

the potential energy of the system.  $K = c\mu_s$  is the linear stiffness coefficient of the

foundation,<sup>10,13</sup> with  $\mu_s$  being the initial shear modulus of the incompressible Neo-

Hookean substrate.  $p$  is the wavenumber of the wrinkling state.  $c = 1 + \lambda_0^2$  and  $\lambda_0$  is

the prestretch ratio of the substrate.  $K_2$  is proportional to the initial shear modulus and depends on the deformation state of the substrate as described in the sequel. The stress function  $F(x, y)$  gives the additional stresses from the fundamental state by

$$N_{\alpha\beta} = F_{,\gamma\gamma} \delta_{\alpha\beta} - F_{,\alpha\beta} \text{ ,} \quad (4)$$

where  $\alpha, \beta, \gamma = 1, 2$  and  $\delta_{\alpha\beta} = \begin{cases} 1, & \alpha = \beta \\ 0, & \alpha \neq \beta \end{cases}$ . In this study, we investigate the cases where the modulus of the film to the substrate is relatively large, e.g. greater than 50. The strain in the film is small. In this case, it is reasonable to assume that the film is linear elastic. Dervaux et al.<sup>19</sup> showed that at low strains, hyperelastic film/substrate systems also satisfy the Foppl-von Karman equation. Our finite element simulations in the sequel also demonstrate that the assumption of the film as linear elastic or hyperelastic basically has no effect on the wrinkling mode evolution when the modulus ratio is relatively large.

Linearizing Eq. (2a) about the pre-buckling state gives the following buckling equation:

$$\frac{1}{12} \bar{E} h^3 \mathcal{W}_{,xxxx} = -h \sigma \mathcal{W}_{,xx} - c \mu_s p \mathcal{W} \text{ ,} \quad (5)$$

where  $\mathcal{W}$  represents the linearized mode. Eq. (5) admits the following solution

$$\mathcal{W} = h A \cos px \text{ ,} \quad (6)$$

where  $A$  refers to the amplitudes of  $\mathcal{W}$ .

Substituting Eq. (6) into (5) gives

$$\sigma = \frac{1}{12} \bar{E} h^2 p^2 + \frac{c\mu_s}{hp} \quad (7)$$

Minimizing Eq. (7) with respect to  $p$  gives

$$p = \frac{1}{h} \left( \frac{6c\mu_s}{\bar{E}} \right)^{1/3}, \quad \delta_c = \frac{\sigma_c}{\bar{E}} = \frac{1}{4} \left( \frac{6c\mu_s}{\bar{E}} \right)^{2/3}. \quad (8)$$

Eq. (8) permits us to determine the critical condition for the onset of sinusoidal wrinkling and has been derived in a previous study.<sup>10</sup> These results will be used in the following wrinkling mode branching analysis.

## 2.2 Wrinkling mode branching

Now consider the sinusoidal wrinkling mode with the additional deflection expressed by

$$w = hb_0 \cos px, \quad (9)$$

with  $b_0$  being the amplitude of wrinkling mode.

Eq. (2) admits the stress function in the following form

$$F = \frac{1}{2} a_1 y^2 + \frac{1}{2} a_2 x^2, \quad (10)$$

where  $a_1$  and  $a_2$  represent the change of average membrane stresses along  $x$  and  $y$  directions, respectively.

Invoking the following compatibility conditions:<sup>8,20</sup>

$$\int_0^l \frac{1}{Eh} (F_{,yy} - \nu F_{,xx}) dx = \int_0^l \frac{1}{2} w_{,x}^2 dx, \quad (11)$$

$$F_{,xx} - \nu F_{,yy} = 0$$

we have

$$a_1 = \frac{1}{4} \bar{E} h^3 b_0^2 p^2, \quad a_2 = \nu a_1. \quad (12)$$

Substituting Eqs. (9) and (10) into the following potential energy function

$$P[w, F] = \frac{1}{2} \int \left[ \frac{1}{12} \bar{E} h^3 w_{,xx}^2 + \frac{1}{Eh} [(1+\nu) F_{,\alpha\beta} F_{,\alpha\beta} - \nu F_{,\gamma\gamma}^2] - h \sigma w_{,x}^2 + 2 \int_0^w R dw \right] dx, \quad (13)$$

we obtain

$$P_1[w, F] = \frac{1}{4} (\sigma_c - \sigma) h^3 p^2 b_0^2 l + \frac{1}{32} \bar{E} h^5 p^4 b_0^4 l. \quad (14)$$

Eq. (13) can be degenerated from the potential energy function given by Cai et al.<sup>8</sup>, and the last term in Eq. (13) refers to the elastic energy of the foundation.

Minimizing the potential energy with respect to  $b_0$ ,  $\partial P_1[w, F] / \partial b_0 = 0$ , it is

obtained that

$$b_0 = \frac{2}{hp} \sqrt{\frac{\sigma - \sigma_c}{\bar{E}}}. \quad (15)$$

Eq. (15) gives the evolution of the wrinkling amplitude and is consistent with the results in previous studies.<sup>21-22</sup> It is interesting to note that the nonlinear term of the

foundation stiffness relevant to  $K_2$  has no influence on the potential energy for this

wrinkling mode when we take the resistant force of the foundation in the form of Eq.

(3) and omit the higher order terms.

We then consider the following period-doubling mode

$$w = h[b_0 \cos px + c_m \sin px / 2], \quad c_m \ll b_0. \quad (16)$$

The stress function is solved from the nonlinear von Karman plate equations as

$$F = \frac{1}{2}a_3y^2 + \frac{1}{2}a_4x^2. \quad (17)$$

From the compatibility condition in Eq. (11), we have

$$a_3 = \frac{1}{4}\bar{E}h^3p^2\left(b_0^2 + \frac{1}{4}c_m^2\right), \quad a_4 = \nu a_3. \quad (18)$$

Inserting Eqs. (16) and (17) into (13) gives the variation of the potential energy of the system from the fundamental state to the period-doubling wrinkling state as

$$\begin{aligned} P_{II}[w, F] = & \frac{1}{4}(\sigma_c - \sigma)h^3p^2b_0^2l + \frac{1}{32}\bar{E}h^5p^4b_0^4l \\ & + \frac{1}{16}\left(\frac{17}{12}\sigma_c - \sigma\right)h^3p^2c_m^2l, \quad (19) \\ & - \frac{3}{16}K_2h^3p^2b_0c_m^2l + \frac{1}{64}\bar{E}h^5p^4b_0^2c_m^2l \end{aligned}$$

where we have neglected the terms of  $c_m^4$ . The increment of the potential energy from

the sinusoidal mode to the period-doubling mode is

$$\begin{aligned} \Delta P = & P_{II} - P_I \\ = & \frac{1}{16}\left[\frac{17}{12}\sigma_c - \sigma\right]h^3p^2c_m^2l \\ & - \frac{3}{16}K_2h^3p^2b_0c_m^2l + \frac{1}{64}\bar{E}h^5p^4b_0^2c_m^2l \end{aligned} \quad (20)$$

Substituting Eq. (15) into (20) gives:

$$\Delta P = \frac{5}{192} h^3 p^2 c_m^2 \sigma_c l - \frac{3}{16} c \mu_s f(\delta, \lambda_0, \delta_c) h^2 p c_m^2 l, \quad (21)$$

where

$$f(\delta, \lambda_0, \delta_c) = h p b_0 \frac{K_2}{K}. \quad (22)$$

$\Delta P = 0$  determines the critical overall compressive strain  $\delta_2$  in the film for the onset of wrinkling pattern transition from sinusoidal to period-doubling, which gives

$$f(\delta_2, \lambda_0, \delta_c) = \frac{5}{24}. \quad (23)$$

It is worth mentioning that Brau et al.<sup>5</sup> have performed an insightful theoretical analysis on the occurrence of the period-doubling mode. They considered an inextensible film with  $\delta_c = 0$  and did not explore the effect of substrate pre-stretch

i.e.,  $\lambda_0 = 1$ . In this case, Eq. (23) degenerates to

$$f(\delta_2) = \frac{5}{24}, \quad (24)$$

where  $f(\delta_2) = 2\sqrt{\delta_2} \frac{K_2}{K}$  according to Eq. (22). Therefore, following the assumption

of Brau et al. and for the case of  $\lambda_0 = 1$ , Eq. (24) gives

$$\delta_2 = \left( \frac{5}{48(K_2 / K)} \right)^2, \quad (25)$$

which is consistent with the result given by Eq. (36) in the supplementary information

of Brau et al.<sup>5</sup>. Eq. (23) indicates that  $\delta_2$  depends on  $\lambda_0$  and  $\delta_c$  as well. Provided that  $K_2$  is known, the function  $f(\delta_2, \lambda_0, \delta_c)$  can be determined and then  $\delta_2$  can be solved from Eq. (23). However, it is, by no means, trivial to determine  $K_2$  analytically. Without considering the substrate compression, Brau et al.<sup>5</sup> have obtained an analytical solution for  $K_2$ , which is zero for an incompressible substrate; with this value,  $\delta_2$  predicted by Eq. (25) will be infinite and inconsistent with nonlinear finite element simulations<sup>10</sup>. Very recently, Hutchinson<sup>13</sup> made an effort to solve  $K_2$ . He also obtained  $K_2=0$  in the absence of substrate compressive deformation. His analysis<sup>13</sup> revealed that  $K_2$  strongly depends on the pre-deformation of the substrate and the boundary condition at the upper surface, for which an analytical solution is difficult to achieve if the realistic interfacial conditions are taken into account. Bearing this in mind, a nonlinear finite element analysis is carried out in this paper to explore the deformation behavior of the substrate at the onset of the period-doubling mode. We will derive an explicit solution to predict  $\delta_2$  without solving  $K_2$  directly.

### 3. Nonlinear finite element analysis

#### 3.1 Computational model

Nonlinear finite element analysis is carried out to investigate the plane strain problem ( $\lambda_{3f} = \lambda_{3s} = 1$ ) of a neo-Hookean bilayer system at compressive strain levels well beyond the bifurcation strain. Our attention is paid to the deformation behavior of the substrate when the wrinkling mode transforms from the sinusoidal to period-doubling. Plane strain finite element simulations are performed via the commercial software ABAQUS.<sup>23</sup> The incompressible neo-Hookean material model is adopted for both the film and the substrate, and the anticipated wavelength is much greater than the element size. The hybrid element (CPE8RH in ABAQUS) is used which is applicable for simulations of incompressible materials.

In the post-buckling analysis, two schemes have been used to introduce the stress-free geometric imperfections to the system to initiate growth of the post-bifurcation modes.<sup>10</sup> With the absence of substrate pre-stretch, a linear perturbation is first accomplished using the “BUCKLE” function in ABAQUS. The critical eigenmode scaled by a very small factor (e.g.  $0.005h$ ) is introduced as a geometric imperfection into the mesh. With the presence of substrate pre-stretch, finite element simulations are first run by specifying a sinusoidal surface deflection at the upper surface. The computed displacement field is then introduced as a stress-free geometric

imperfection into the mesh. Displacement-controlled loading is employed with  $u_1$  (independent of  $x_2$ ) and zero shear traction specified on the vertical sides of the model. The nominal compressive overall strain imposed to the system after the film is attached to the substrate,  $\delta$ , is defined in terms of the film stretch,  $\lambda_{1f}$ , calculated from the relative difference between  $u_1$  on the two sides of the model. The displacement  $u_2$  and the shear traction on the bottom surface of the model are taken to be zero. The computational model has a width on the order of 10 wavelengths of the sinusoidal wrinkling mode. The depth of the substrate is taken to be more than 10 times the sinusoidal wavelength and, thus, sufficiently deep such that the substrate can be regarded as infinite. To capture the occurrence of the period-doubling mode and the deformation behavior of the substrate at the bifurcation strain, both loading and unloading procedures are explored. The unloading procedure permits to identify the critical overall strain for the onset of period-doubling mode more accurately.

### *3.2 A characteristic strain at the onset of period-doubling mode*

Fig. 3 shows a sequence of substrate deformations in both loading and unloading for the case without substrate pre-stretch (also see Video 1 in Supplementary Information). The computational results reveal a characteristic

strain of  $\varepsilon_c=0.36$  (point g) in the deformed substrate at the onset of period-doubling mode. The characteristic strain  $\varepsilon_c$  is the maximum nominal compressive strain in the substrate along the loading direction (Fig. 3). We use the following criterion to identify  $\varepsilon_c$ . Fig. 4(a, b) shows the sinusoidal wrinkling and the period-doubling mode, respectively. We determine the bifurcation point for the onset of period-doubling mode by examining the relative amplitude difference at the trough of waves. We carefully examine the wave amplitudes at  $A_1, A_2, A_3$  and  $B_1, B_2$  in Fig. 4. For the sinusoidal wrinkling mode, the amplitudes of points  $A_i$  are basically the same as those of  $B_j$ . However, with the appearance of the period-doubling mode, the symmetry is broken. To determine the bifurcation point, we define the difference between the average value of the wave amplitudes at  $A_1, A_2, A_3$  and that at  $B_1$  and  $B_2$  as

$$\xi = \left| \frac{\frac{1}{3}(D_{A_1} + D_{A_2} + D_{A_3}) - \frac{1}{2}(D_{B_1} + D_{B_2})}{\frac{1}{3}(D_{A_1} + D_{A_2} + D_{A_3})} \right|, \quad (26)$$

where  $D_{A_i}$  ( $i=1, 2, 3$ ) and  $D_{B_j}$  ( $j=1,2$ ) are the amplitudes at points  $A_i$  and  $B_j$ , respectively. An illustrative example without prestretch is shown in Fig. 5, where the modulus ratio is 448. It is clearly seen when the overall compressive amount is beyond 0.17,  $\xi$  increases quickly. Thus in this case,  $\delta=0.17$  is taken as the critical overall compressive strain for the onset of period-doubling mode, and the

corresponding maximum nominal strain in the substrate is around 0.36, as indicated in Fig. 5. However, it should be pointed that the transition of the amplitude difference is smooth in Fig. 5. In this sense, an exact determination of the critical overall strain is difficult, but indeed the value of 0.17 is a good approximation.

Our analysis shows that the characteristic strain  $\varepsilon_c$  is basically independent of the modulus ratio of the film to the substrate and insensitive to the geometric imperfection introduced in the system, as shown in Fig. 6. The parameter  $\eta$  in Fig. 6 represents the ratio of the imperfection amplitude to the film thickness. The value of  $\varepsilon_c$  is very close to the crease strain identified by Hong et al.<sup>7</sup> and Hohlfeld and Mahadevan.<sup>9</sup> This may imply that the substrate nonlinear instability plays a dominant role in the occurrence of the period-doubling mode in film/substrate bilayer systems.

We also explore the case with substrate pre-stretch, i.e.,  $\lambda_0 \neq 1$ . Our results show that  $\varepsilon_c$  slightly depends on  $\lambda_0$ . When  $\lambda_0$  changes from 0.8 to 1.2,  $\varepsilon_c$  varies from 0.34 to 0.38; and in this case  $\varepsilon_c=0.36$  is still a reasonable approximation.

The characteristic strain identified here may not only help understand the physics behind the occurrence of period-doubling mode and localized folding in bilayer systems, but also provide a means to determine the critical overall compressive strain at the onset of wrinkling mode transition. This issue will be further

addressed below.

#### 4. Explicit solutions to predict the critical overall strain for the onset of period-doubling mode

In this section, we show the characteristic strain identified in Section 3 permits to determine  $\delta_2$  in an explicit form. Our analysis reveals that  $\delta_2$  depends on  $\lambda_0$  and

$\delta_c$ , i.e.,

$$\delta_2 = f_1(\lambda_0, \delta_c). \quad (27)$$

Without substrate prestretch, i.e.,  $\lambda_0 = 1$

$$\delta_2 = f_1(\delta_c). \quad (28)$$

Based on the characteristic strain identified in Section 3, we provide a means to determine the function  $f_1$  and  $\delta_2$  in Eq. (28). For the sinusoidal wrinkling mode, the maximum nominal strain  $\varepsilon_{11,\max}$  along the loading direction depends on  $\delta_c$  and the overall compressive strain  $\delta$  without substrate prestretch (Fig. 7).

When  $\varepsilon_{11,\max}$  reaches  $\varepsilon_c$ ,  $\delta$  will have the value of  $\delta_2$ , i.e.,

$$\varepsilon_{11,\max} = \varepsilon_c = 0.36 = g(\delta_2, \delta_c). \quad (29)$$

Therefore, provided that the function  $g$  is known, we can determine the function  $f_1$  in Eq. (28). Based on the theoretical analysis and nonlinear finite element simulations in Section 2, we have determined the function  $g$ . The function  $g$  gives the correlation among  $\varepsilon_{11,\max}$ ,  $\delta$  and  $\delta_c$  as

$$\varepsilon_{11,\max} = g(\delta, \delta_c) = 1.08 \left( \delta - \frac{1}{2} \delta^2 - \delta_c + \frac{1}{2} \delta_c^2 \right)^{3/5} + \delta_c. \quad (30)$$

The last term in Eq. (30) ensures that  $\varepsilon_{11,\max} = \delta_c$  when  $\delta = \delta_c$ . For illustration, the function  $g$  determined from a finite element example is shown in Fig. 8.

From Eqs. (29) and (30),  $\delta_2$  is derived in the explicit form:

$$\delta_2 = 1 - \sqrt{(1 - \delta_c)^2 - 2 \left( \frac{\varepsilon_c - \delta_c}{1.08} \right)^{5/3}}, \quad (31)$$

indicating that the dependence of  $\delta_2$  on  $\delta_c$  is rather weak when the modulus ratio

$\mu_f / \mu_s$  is large. For instance, when  $\mu_f / \mu_s > 50$ , Eq. (31) gives  $\delta_2 \approx 0.175$ , as shown

in Fig. 9. Fig. 10 shows that  $\delta_2$  is insensitive to the geometric imperfections introduced in the post-buckling analysis. The solution given by Eq. (31) is consistent with the experimental results of Brau et al.<sup>5</sup> and finite element simulations.<sup>10</sup>

In the case of  $\lambda_0 \neq 1$ , our theoretical analysis shows that  $\delta_2 = f_1(\lambda_0, \delta_c)$ , and the

prestrain in the substrate is  $\delta_0 = 1 - \lambda_0$ . In the presence of prestretch, the maximum (nominal) compressive strain in the substrate is given by

$$\varepsilon_{11,\max}^* = \delta_0 + \varepsilon_{11,\max} (1 - \delta_0). \quad (32)$$

When  $\varepsilon_{11,\max}^* = \varepsilon_c$ , period-doubling mode occurs. This condition together with Eqs. (30)-(32) gives

$$\delta_2 = 1 - \sqrt{(1 - \delta_c)^2 - 2 \left[ \frac{(\varepsilon_c - \delta_0) / (1 - \delta_0) - \delta_c}{1.08} \right]^{5/3}}. \quad (33)$$

We have compared the predicted  $\delta_2$  given by Eq. (33) with finite element simulations. The results are plotted in Fig. 11 for two different modulus ratios and various prestretch ratios. Eq. (33) matches the finite element results well. It is also seen that the prestretch has pronounced effects on  $\delta_2$ . With the increase of  $\lambda_0$  from 0.75 to 1.25,  $\delta_2$  changes almost ten times.

The solution in Eq. (33) allows us to predict the critical condition for the onset of period-doubling mode, and thus it provides a guideline for controlling surface wrinkling patterns by tuning the stress state in the substrate. Understanding the morphogenesis and origin of shapes has long been a central goal of developmental biology.<sup>24-26</sup> Growth is responsible for the morphogenesis of biological organs and tissues, which consists of a series of orchestrated steps.<sup>27</sup> Besides genetic and

chemical effects, mechanical environments play a significant role in regulating the pattern formation. Differential growth or atrophy of tissues and organs could induce residual stresses, which are important to the morphogenesis and physiological functions of soft tissues and organs.<sup>25, 28-30</sup> Recently, Ben Amar and Jia<sup>31</sup> have studied the surface wrinkling and the zigzag mode of a hyper-elastic bilayer soft tissue. In their study, differential growth of the soft tissue elicits the residual stresses which lead to surface instability. In this paper, we study the occurrence of a period-doubling mode in the plane strain compression of film/substrate bilayer systems with focus on the effects of prestresses. Eq. (33) clearly demonstrates that prestresses in the substrate affect the evolution of wrinkling patterns, and therefore it would be interesting to take this factor into account in understanding the correlation between the growth and morphogenesis of biological organs and tissues.

It should be pointed out that this study is limited to the system with a flat surface. In this sense, although Fig. 10 shows that  $\delta_2$  is insensitive to the geometric imperfections introduced in the post-buckling analysis, the geometric imperfections should be smaller than the film thickness in order to appropriately use Eqs. (31) or (33). To further illustrate this point, we explore a case where the geometric imperfections are introduced based on a buckled deformation corresponding to the sinusoidal mode. In the initial configuration, the buckled amplitude of film is much greater than its thickness. Video 2 in the Supplementary Information shows the deformed configurations of the system at different overall compressive strains. In this

case, Eq. (31) is no longer valid to predict the critical overall compressive strain  $\delta_2$  for the onset of period-doubling mode. However, it is interesting to find that the period-doubling still occurs when the local nominal strain in the substrate at the center of the peak (Fig. 7) reaches the characteristic strain  $\varepsilon_c$ . Both this example and the solution in Eq. (31) indicate that the period-doubling mode uses the sinusoidal wrinkled mode as the base state and is almost independent of the overall strain in the fundamental state given in Fig. 2. Besides the wavelength, the sinusoidal wrinkling mode is primarily characterized by its amplitude. This may help understand why the critical condition for period doubling is given in terms of the characteristic maximum nominal strain in the substrate.

## 5. Concluding Remarks

Understanding the unusual wrinkling modes at compressive strains well above the bifurcation strain such as period doubling and folding<sup>5,10,15,31</sup> represents a challenging issue. In this paper, we have studied the occurrence of a period-doubling mode in the plane strain compression of film/substrate bilayer systems. Our theoretical analysis shows that the overall compressive strain  $\delta_2$  in the film for the onset of the period-doubling mode depends on the substrate prestretch ratio and the critical overall strain for the onset of wrinkling. When the modulus ratio of the film to the substrate is large,

say greater than 50,  $\delta_2$  only depends on the substrate prestretch and is basically independent of the wrinkling strain. Nonlinear finite element analysis (compressing and unfolding the system) reveals a characteristic strain of 0.36 for the onset of period-doubling mode, which is close to the critical strain at which crease sets in. This indicates that the period-doubling mode may be the consequence of the nonlinear instability of the substrate. Finally, explicit solutions based on the characteristic strain have been developed to predict the overall compressive strain for the onset of the period-doubling mode in the cases with or without substrate prestretch. The solutions proposed here match both experimental and finite element results well.

### **Acknowledgment**

YPC acknowledges the supports from the National Natural Science Foundation of China (Grant No. 11172155), Tsinghua University and 973 Program of MOST (2010CB631005). We acknowledge the valuable and insightful comments and remarks from Prof. John W. Hutchinson (Harvard University) on the issue addressed here.

## References

- 1 N. Bowden, S. Brittain, A. G. Evans, J. W. Hutchinson and G. M. Whitesides, *Nature*, 1998, **393**, 146.
- 2 J. Genzer and J. Groenewold, *Soft Matter*, 2006, **2**, 310.
- 3 I. Tokarev and S. Minko, *Soft Matter*, 2009, **5**, 511.
- 4 X. Chen and J. Yin, *Soft Matter*, 2010, **6**, 5667.
- 5 F. Brau, H. Vandeparre, A. Sabbah, C. Poulard, A. Boudaoud and P. Damman, *Nat. Phys.*, 2011, **7**, 56.
- 6 B. Li, Y. P. Cao, X. Q. Feng and H. J. Gao, *Soft Matter*, 2012, **8**, 5728.
- 7 W. Hong, X. Zhao and Z. Suo, *Appl. Phys. Lett.*, 2009, **95**, 111901.
- 8 S. Cai, D. Breid, A.J. Crosby, Z. Suo, J. W. Hutchinson, *J. Mech. Phys. Solids*, 2011, **59**, 1094.
- 9 E. Hohlfeld and L. Mahadevan, *Phys. Rev. Lett.*, 2011, **106**, 105702.
- 10 Y. P. Cao and J. W. Hutchinson, *J. App. Mech.*, 2012, **79**, 031019.
- 11 J. F. Zang, X. Zhao, Y. P. Cao and J. W. Hutchinson, *J. Mech. Phys. Solids*, 2012, **20**, 1265.
- 12 Y. P. Cao and J. W. Hutchinson, *Proc. R. Soc. A*, 2012, **468**, 94.
- 13 J. W. Hutchinson, *Phil. Trans. R. Soc. A*, 2013, **371**, 1993.
- 14 M. A. Biot, *Appl. Sci. Res.*, 1963, **12**, 168.
- 15 J. Y. Sun, S. Xia, M. Y. Moon, K.H. Oh and K. S. Kim, *Proc. Roy. Soc. A*, 2012, **468**, 932-953.
- 16 Y. Ebata, A. B. Croll and A. J. Crosby, *Soft Matter*, 2012, **8**, 9086-9091.
- 17 S. P. Timoshenko, and J. M. Gere, *Theory of Elastic Stability*, McGraw-Hill, New York, 1961.
- 18 W. T. Koiter, In: van der Heijden, A.M.A. (Ed.), *Elastic Stability of Solids and Structures*. Cambridge University Press, Cambridge, 2009.
- 19 J. Dervaux, P. Ciarletta and M. Ben Amar, *J. Mech. Phys. Solids*, 2009, **57**, 458-471.
- 20 X. Chen and J. W. Hutchinson, *J. App. Mech.*, 2004, **71**, 597.
- 21 R. Huang, *J. Mech. Phys. Solids*, 2005, **53**, 63-89.

- 22 Z. Y. Huang, W. Hong and Z. Suo, *J. Mech. Phys. Solids*, 2005, **53**, 2101-2118.
- 23 ABAQUS analysis user's manual, Version 6.8, 2008.
- 24 E. Sharon, M. Marder and H. L. Swinney, *Am. Sci.*, 2004, **92**, 254-261.
- 25 H. Liang and L. Mahadevan, *Proc. Natl. Acad. Sci.*, 2009, **106**, 22049-22054.
- 26 D. W. Thompson, *On growth and form*, Cambridge University Press, 1942.
- 27 L. A. Taber, *App. Mech. Rev.*, 1995, **48**, 487-545.
- 28 A. Goriely and M. Ben Amar, *Phys. Rev. Lett.*, 2005, **94**, 198103.
- 29 J. Dervaux and M. Ben Amar, *Phys. Rev. Lett.*, 2008, **101**, 68101.
- 30 B. Li, Y. P. Cao, X. Q. Feng and H. Gao, *J. Mech. Phys. Solids*, 2011, **59**, 758-774.
- 31 M. Ben Amar and F. Jia, *Proc. Natl. Acad. Sci.*, 2013, **110**, 10525-10530.

## Figure Captions

**Fig. 1** Period-doubling mode observed in the experiments of Brau et al.<sup>5</sup>; (a) Period-doubling mode; (b) Wrinkling morphology of the film at the overall compressive strain of 0.19 .

**Fig. 2** Compression induced surface wrinkling in film/substrate bilayer system.

**Fig. 3** Evolution of wrinkling patterns in the compression and unfolding the bilayer system. When the period-doubling mode occurs, the maximum nominal strain in the substrate along the loading direction is around 0.36.

**Fig. 4** (a) Sinusoidal wrinkling; (b) Period-doubling mode, the amplitudes at points  $A_1$ ,  $A_2$ ,  $A_3$ ,  $B_1$  and  $B_2$  are used to determine the bifurcation point for the onset of period-doubling mode.

**Fig. 5** Variation of the parameter  $\xi$  and the maximum nominal strain  $\varepsilon_{11,\max}$  in the substrate with the overall compressive strain  $\delta$ . When  $\delta$  is beyond 0.17, the parameter  $\xi$  increases quickly, indicating period-doubling mode occurs; at this moment,  $\varepsilon_{11,\max}$  in the substrate along loading direction is around 0.36.

**Fig. 6** The characteristic strain is basically a constant for different modulus ratios, (a); and not sensitive to the imperfection amplitudes, (b).

**Fig. 7** The maximum nominal strain  $\varepsilon_{11,\max}$  in the substrate along loading direction depends on the critical overall strain and the wrinkling strain.

**Fig. 8** Function  $g$  with respect to the overall compressive strain, where we take

$$\mu_f / \mu_s = 448 .$$

**Fig. 9** Comparison of  $\delta_2$  predicted from Eq. (31) for different modulus ratios with our finite element results and experimental results in the literature.<sup>5</sup>

**Fig. 10** The critical overall strain  $\delta_2$  for the onset of period-doubling mode corresponding to different imperfection amplitudes.

**Fig. 11** Comparison of  $\delta_2$  predicted from Eq. (33) for different prestretch ratios with finite element results. (a) modulus ratio  $\mu_f / \mu_s = 448$ ; (b) modulus ratio

$\mu_f / \mu_s = 774$ .

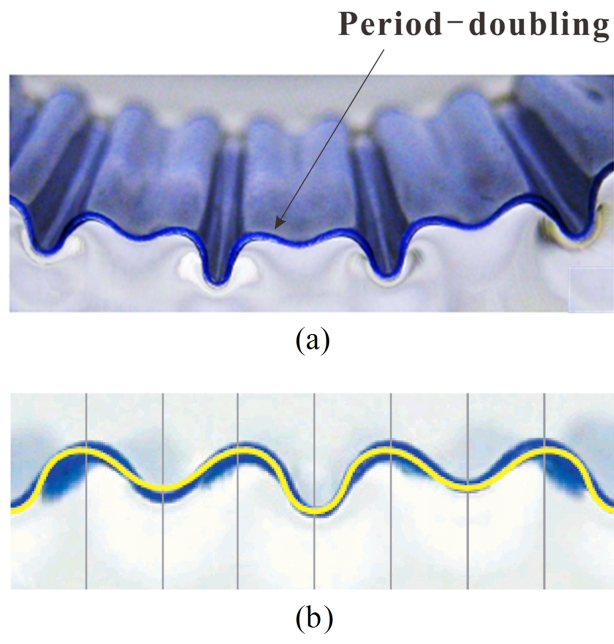


**Figure 1**

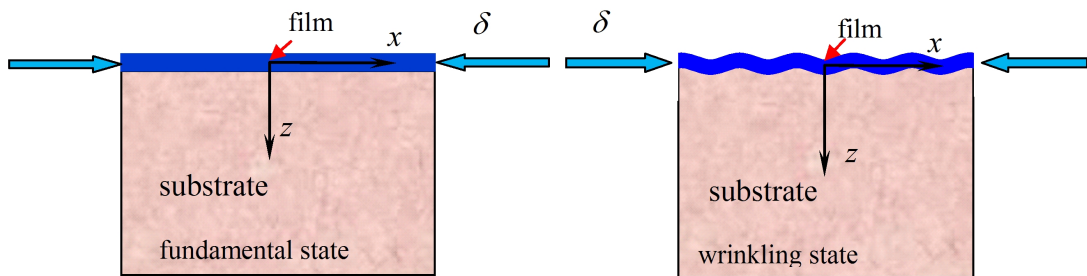


**Figure 2**

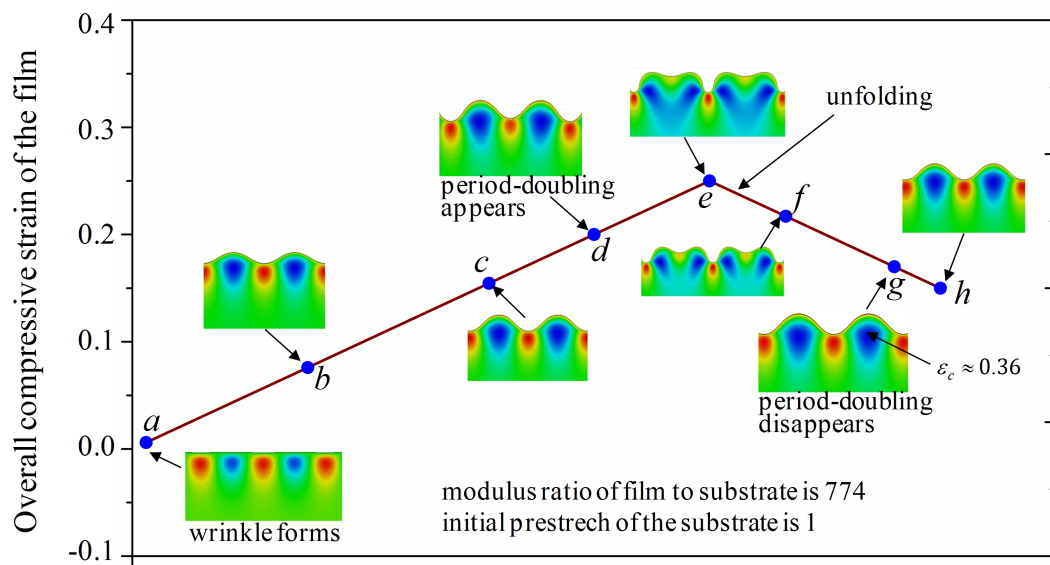


**Figure 3**

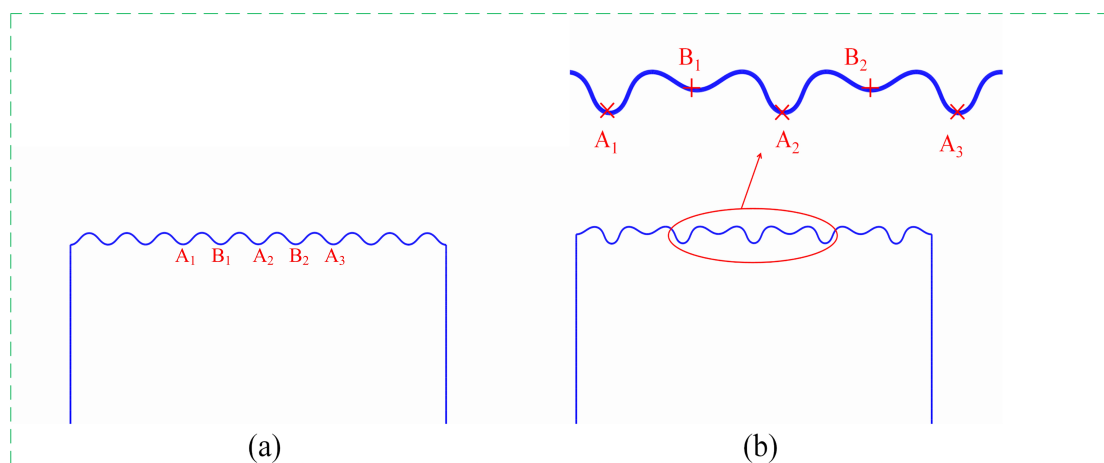


**Figure 4**

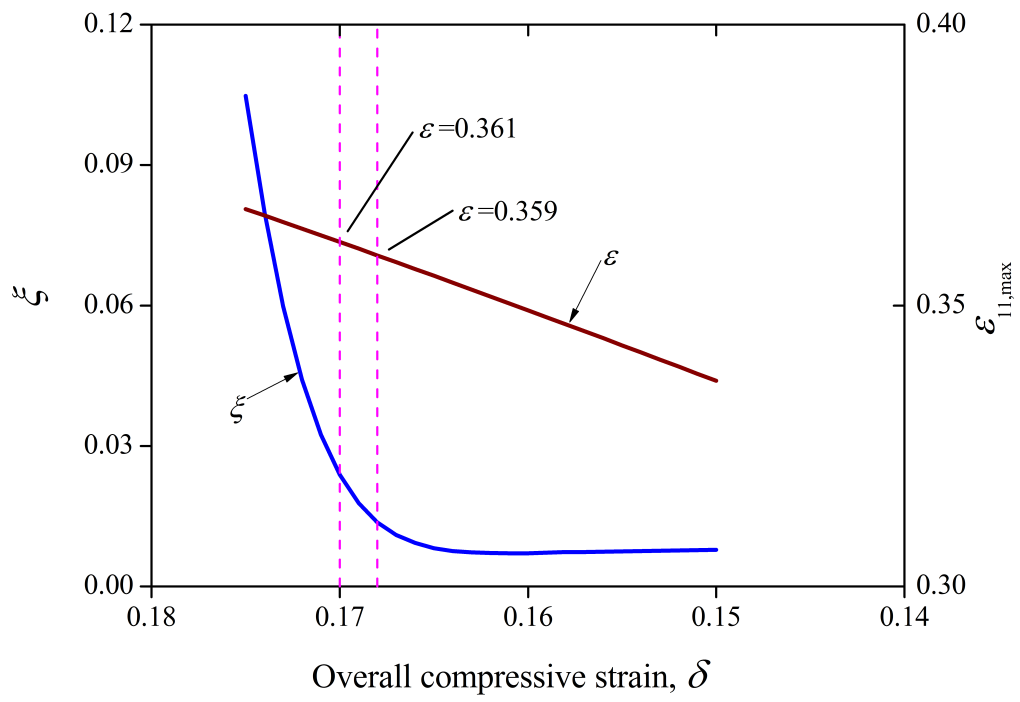
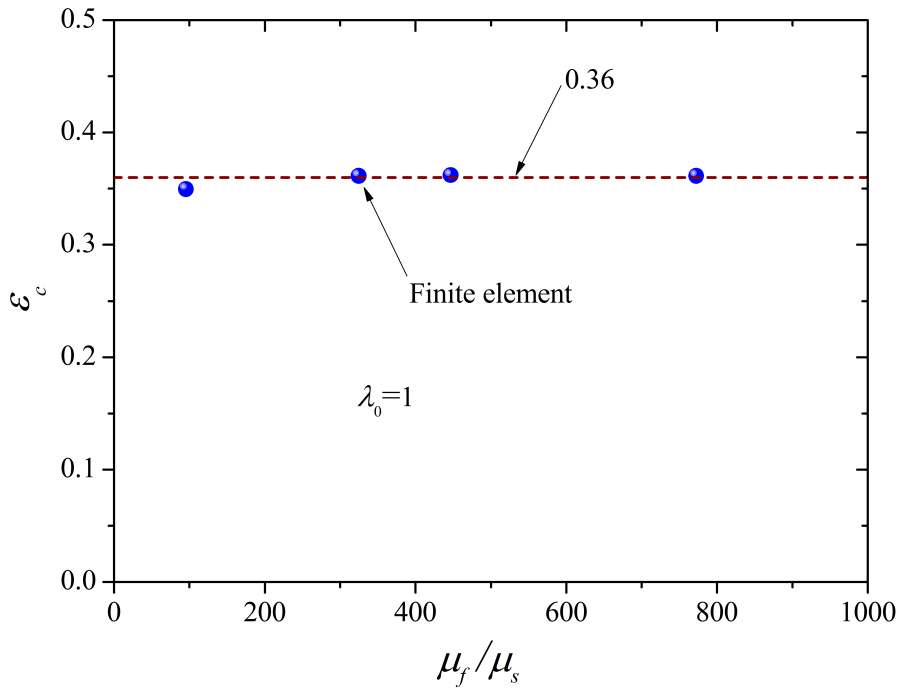
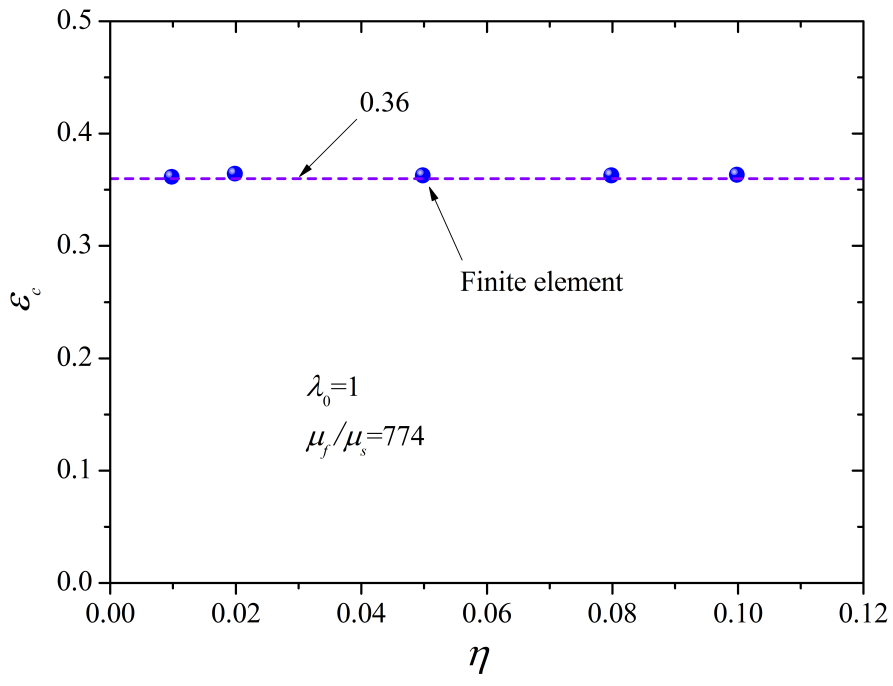


**Figure 5**



(a)



(b)

Figure 6

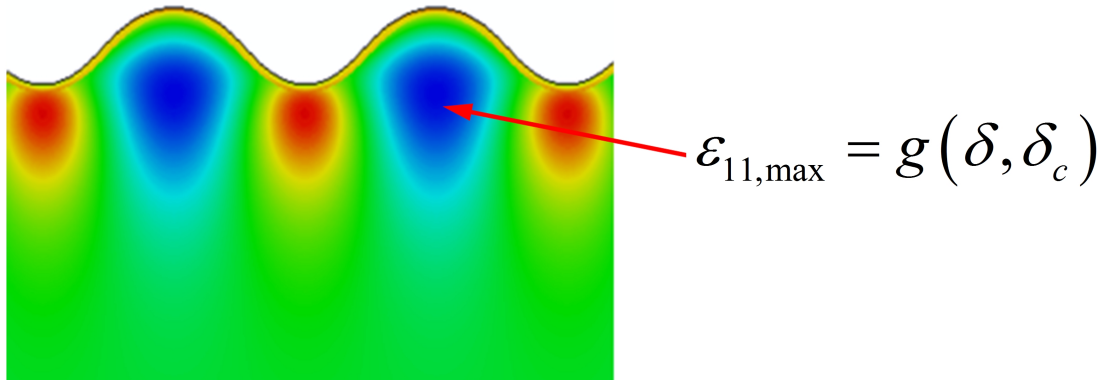


**Figure 7**

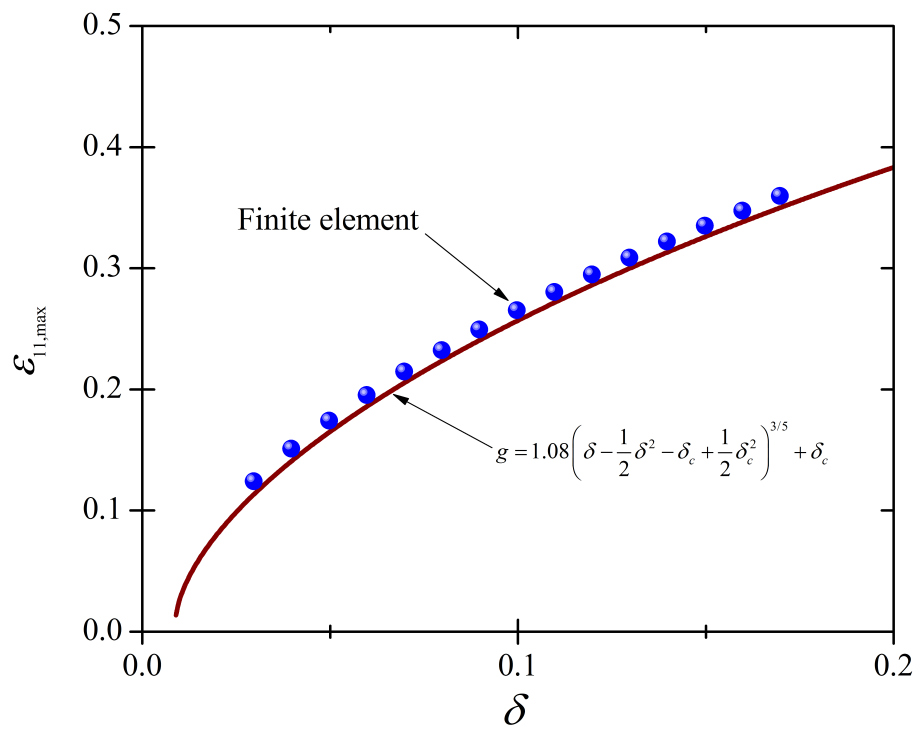


**Figure. 8**

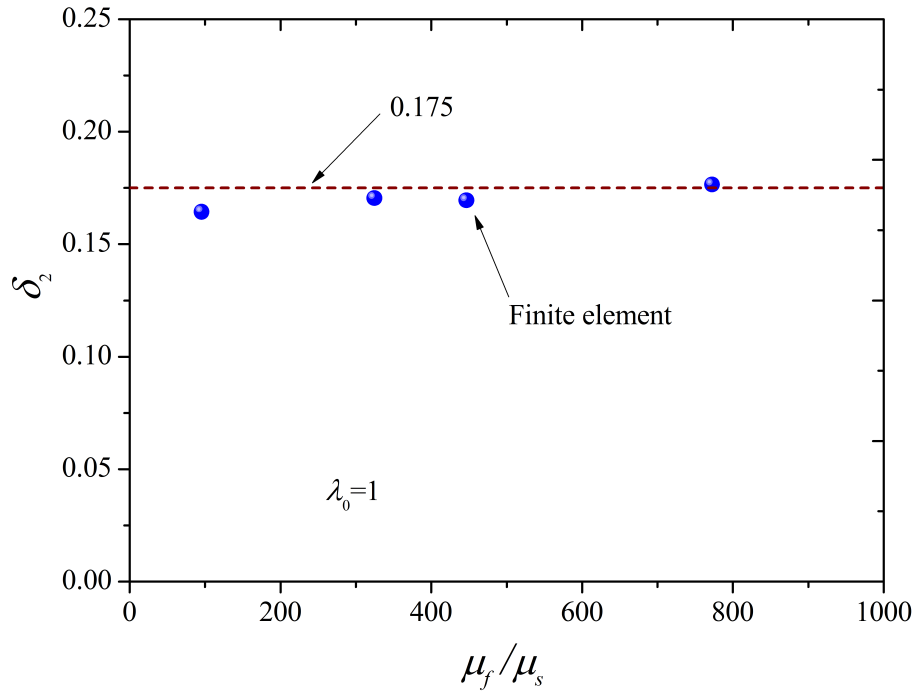


Figure 9

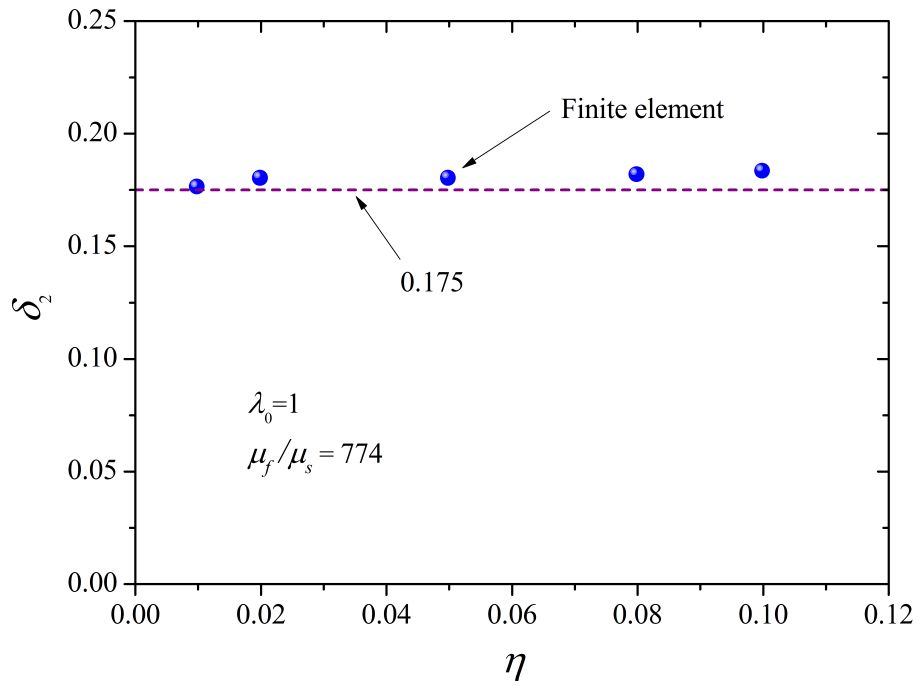
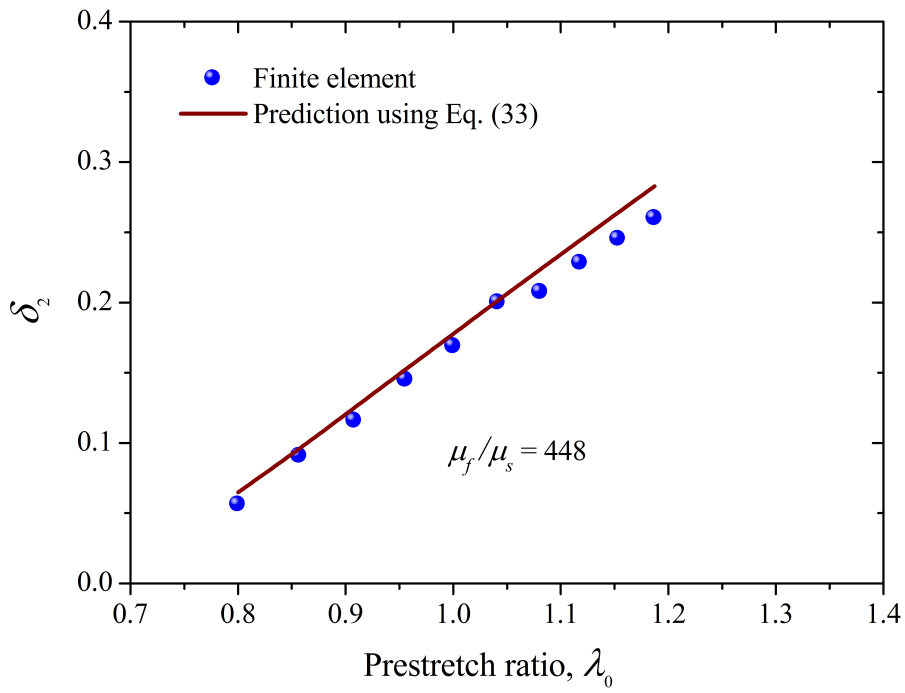
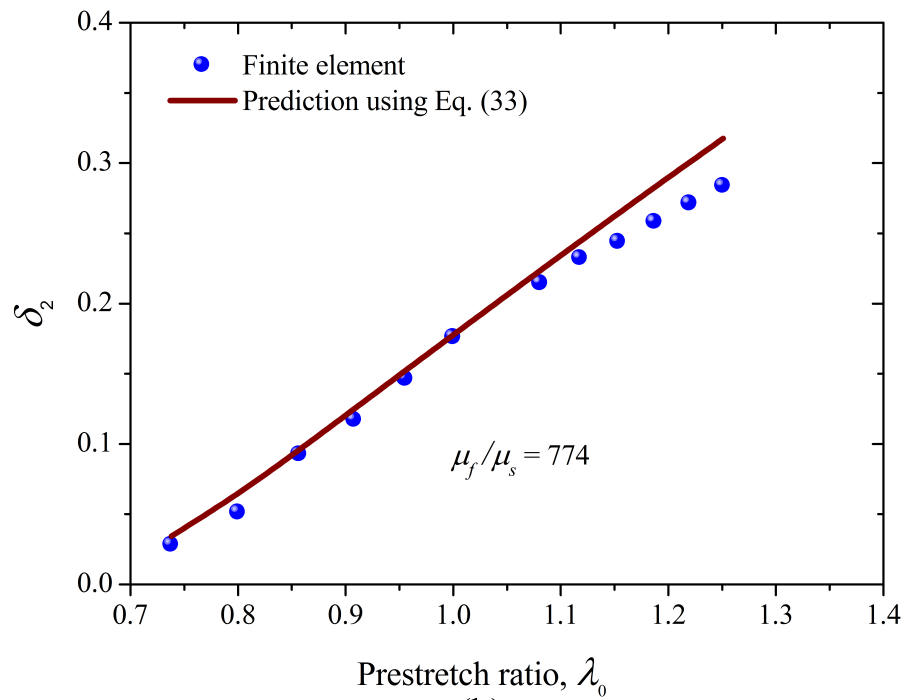


Figure 10



(a)



(b)

Figure 11